Local magnetic properties of La0.83Sr0.17Mn0.9Fe0.1−xZnxO3

Zakir Y. Seidov, Ivan V. Yatsyk, Farit G. Vagizov, Vladimir Alekseevich Shustov, A. G. Badelin, V. K. Karpasyuk, M. J. Najafzade, I. N. Ibrahimov, Svetlana Kh. Estemirova, Hans-Albrecht Krug von Nidda, Rushana M. Eremina

Angaben zur Veröffentlichung / Publication details:

Seidov, Zakir Y., Ivan V. Yatsyk, Farit G. Vagizov, Vladimir Alekseevich Shustov, A. G. Badelin, V. K. Karpasyuk, M. J. Najafzade, et al. 2022. "Local magnetic properties of La0.83Sr0.17Mn0.9Fe0.1−xZnxO3." *Journal of Magnetism and Magnetic Materials* 552: 169190. https://doi.org/10.1016/j.jmmm.2022.169190.

Local magnetic properties of $La_{0.83}Sr_{0.17}Mn_{0.9}Fe_{0.1-x}Zn_xO_3$

Z.Y. Seidov [a,f], I.V. Yatsyk [b], F.G. Vagizov [c], V.A. Shustov [b], A.G. Badelin [d], V.K. Karpasyuk [d], M.J. Najafzade [a], I.N. Ibrahimov [a], S.Kh. Estemirova [e], H.-A. Krug von Nidda [f,*], R.M. Eremina [b]

[a] *Institute of Physics, Azerbaijan National Academy of Sciences, AZ-1143 Baku, Azerbaijan*
[b] *Zavoisky Physical-Technical Institute, Federal Research "Kazan Scientific Center of RAS", Kazan, 420029, Russia*
[c] *Institute of Physics, Kazan Federal University, 420008, Russia*
[d] *Astrakhan State University, 414056 Astrakhan, Russia*
[e] *Institute for Metallurgy, Ural Division of RAS, 620016, Yekaterinburg, Russia*
[f] *Experimental Physics V, Center for Electronic Correlations and Magnetism, Institute of Physics, University of Augsburg, D-86135 Augsburg, Germany*

A B S T R A C T

Magnetic properties of polycrystalline $La_{0.83}Sr_{0.17}Mn_{0.9}Fe_{0.1-x}Zn_xO_3$ ($x = 0$, $x = 0.05$) have been investigated by means of electron spin resonance, magnetic susceptibility, and Mössbauer measurements. Both samples show a clear ferromagnetic transition. The Curie temperature T_C decreases on increasing Fe content. Mössbauer studies indicate that Fe in these compounds is in the trivalent high-spin state. The temperature evolution of the Mössbauer spectra at low temperatures ($T < T_C$) is typical for ferromagnetic clusters with a wide distribution in size and magnetic correlation length. The inverse susceptibility of all the samples deviates from the Curie–Weiss law above T_C, indicating the presence of fluctuations on approaching magnetic order. An anomalous downturn of the inverse susceptibility for $x = 0.05$ significantly above T_C and the concomitant observation of ferromagnetic resonance signals coexisting with the paramagnetic resonance up to approximately room temperature, is caused by a Griffiths-like behavior. This regime is characterized by the coexistence of ferromagnetic entities within the globally paramagnetic phase.

1. Introduction

Perovskite manganese oxides, which possess the general chemical formula $R_{1-x}A_xMnO_3$ (R and A denote rare- and alkaline-earth elements, respectively) have attracted broad research interest due to their unusual transport and magnetic properties, which are indispensable for applications in spintronic devices [1–8]. These fascinating properties including metal–insulator transitions, colossal magnetoresistance (CMR), and magneto-caloric effects, arise due to strong coupling between the spin, charge, orbital, and lattice degrees of freedom and corresponding ordering phenomena [9,10]. Correlation between them results in significant changes from antiferromagnetic (AFM) to ferromagnetic (FM) order and from insulating to metallic behavior. The coexistence and competition between the double exchange (DE) and super-exchange (SE) interaction is related to FM and AFM properties in manganites, respectively [8,11,12]. One of the peculiar phenomena that can be observed in manganites, is the existence of a Griffiths-like phase. Numerous studies have shown that the occurrence of a Griffiths phase (GP) [13] in magnetic systems may have many different origins [14–19], most of the GP compounds are known to exhibit bulk FM order.

The Griffiths theory was originally developed for diluted Ising ferromagnetic materials [13]. It was found that a new phase, which represents ferromagnetic clusters in a paramagnetic matrix, shows up in such systems above the Curie temperature. Griffiths showed that the essential singularity develops in a temperature range $T_C(p) < T < T_G$, where p is the disorder parameter due to dilution of ferromagnetic bonds and $T_G = T_C(0)$ is the new transition temperature corresponding to the Curie temperature of the undiluted Ising ferromagnet. This phase regime is usually referred to as the Griffiths phase. An infinite ferromagnetic cluster is formed in the paramagnetic regime below the so-called Griffiths temperature T_G. This infinite cluster exists down to the ferromagnetic phase-transition temperature $T_C(p)$, which due to dilution of ferromagnetic bonds decreases on increasing disorder parameter p.

The occurrence of a Griffiths-type phase in manganites is confirmed by a number of experimental facts, e.g., the detection of a weak ferromagnetic resonance (FMR) signal above the Curie temperature T_C coexisting with the electron paramagnetic resonance signal [20–25] as well as the appearance of a temperature regime above T_C with an atypical behavior for purely FM or paramagnetic phases in the magnetic susceptibility [26–31].

* Corresponding author.
E-mail address: hans-albrecht.krug@physik.uni-augsburg.de (H.-A. Krug von Nidda).

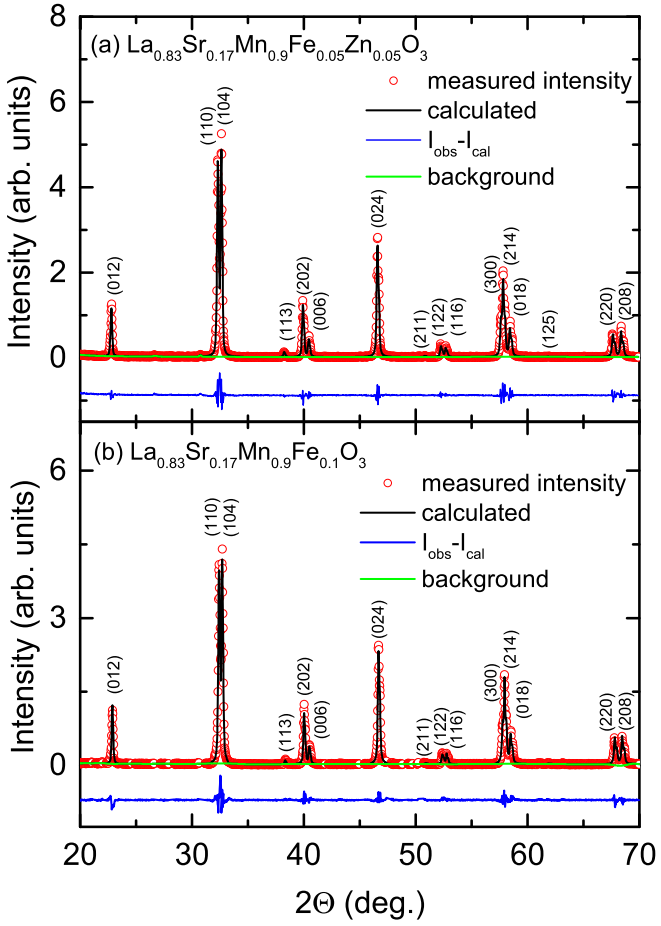

Fig. 1. X-ray diffraction patterns of $La_{0.83}Sr_{0.17}Mn_{0.9}Fe_{0.1-x}Zn_xO_3$ ceramic samples at room temperature for (a) $x = 0.05$ and (b) $x = 0$.

$La_{1-x}A_xMn_{1-y}Fe_yO_3$ (A = Ca, Sr) belongs to a family of hole-doped mixed-valence manganite perovskites, exhibiting a CMR effect and magneto-caloric effect [32–34]. The compounds are obtained by substitution of Fe for Mn in $La_{1-x}A_xMnO_3$ (A = Ca, Sr) [33–35]. The hole doping of manganite perovskites, realized by substitution of a divalent element for La^{3+}or by formation of cation vacancies, results in a fraction of Mn^{4+} ions on the Mn^{3+} sites [8]. The $Mn^{3+,4+}$ mixed valence leads to FM Mn^{3+}–Mn^{4+} DE interactions, competing with AFM Mn^{3+}–Mn^{3+} SE interactions [8]. The case of Fe is particularly interesting because of the large extent to which it can replace Mn due to similar ionic radii of Fe^{3+} and Mn^{3+}. The magnetic investigations of $La_{1-x}Sr_xMn_{1-y}Fe_yO_3$ (with x=0.3 and y=0.15–0.25) and $La_{1-x}Ca_xMn_{1-y}Fe_yO_3$ (with x=0.37 and y=0–0.18) compounds shows that FM Curie temperature T_C in both systems decreases with increasing y [33,35]. Such behavior of transition temperature T_C is connected with weakening of the double-exchange FM interaction by Fe doping. In this article we present X-ray diffraction, magnetization, electron spin resonance (ESR) and Mössbauer experiments on polycrystalline samples of $La_{0.83}Sr_{0.17}Mn_{0.9}Fe_{0.05}Zn_{0.05}O_3$ and $La_{0.83}Sr_{0.17}Mn_{0.9}Fe_{0.1}O_3$. Our results indicate the important role of magnetic cluster formation both in the FM ordered and in the paramagnetic phase. Especially in the latter one, the Griffiths phase can be tuned by the balance of disorder (Zn^{2+}) and AFM interactions (Fe^{3+}).

2. Sample preparation and characterization

Polycrystalline samples of $La^{3+}_{0.83}Sr^{2+}_{0.17}Mn^{3+}_{0.73-x}Mn^{4+}_{0.17+x}Fe^{3+}_{0.1-x}Zn^{2+}_xO^{2-}_3$ with $x = 0$ and $x = 0.05$ were synthesized by traditional ceramic processing, including two grindings in a ball mill with addition of alcohol and preliminary burning at 1273 K for 4 h. The final sintering step was performed in air at 1473 K for 10 h, and the samples were cooled together with the furnace. In order to provide stoichiometric oxygen content ($\delta = 0$), the samples were annealed at 1223 K and partial pressure of oxygen in the gas phase $p_{O_2} = 10^{-1}$ Pa. The choice of annealing conditions was based on the data of Ref. [36]. Annealing was carried out for 96 h. Phase composition and unit-cell parameters were determined by powder X-ray diffraction at room temperature (diffractometer Shimadzu XRD-7000, Cu K_α radiation). The X-ray diffraction analysis of the synthesized manganites $La_{0.83}Sr_{0.17}Mn_{0.9}Fe_{0.05}Zn_{0.05}O_3$ and $La_{0.83}Sr_{0.17}Mn_{0.9}Fe_{0.1}O_3$ showed that both compounds are single-phase and the structure of the samples belongs to the proper space group $R\bar{3}c$. The diffraction patterns of the samples are shown in Fig. 1(a,b). The corresponding unit-cell parameters presented in Table 1, were determined and refined using the Maud-v2.94 program package [37,38].

Table 1
Crystallographic data for $La_{0.83}Sr_{0.17}Mn_{0.9}Fe_{0.1-x}Zn_xO_3$ (x=0, x=0.05).

Compound	Cryst.str.	a (Å)	c (Å)	α (°)	β (°)	γ (°)
$x = 0.05$	$R\bar{3}c$	5.537	13.3743	90	90	120
$x = 0$	$R\bar{3}c$	5.5243	13.3611	90	90	120

3. Results and discussion

3.1. Magnetic susceptibility and magnetization

Magnetization measurements were performed using a superconducting quantum interference device (SQUID) magnetometer MPMS5 (Quantum Design) in magnetic fields up to $H \leq 50$ kOe for the temperature regime $1.8 \leq T \leq 400$ K. Figs. 2 and 3 show the temperature dependence of magnetic susceptibility and its inverse for the compounds $La_{0.83}Sr_{0.17}Mn_{0.9}Fe_{0.05}Zn_{0.05}O_3$ and $La_{0.83}Sr_{0.17}Mn_{0.9}Fe_{0.1}O_3$. The Curie temperature T_C, defined as the one corresponding to the peak of $d\chi/dT$ in the χ vs T curve (see Insets in Fig. 2 and 3), amounts to $T_C(x = 0.05) = 208$ K and $T_C(x = 0) = 151$ K, respectively (Table 2).

The temperature dependence of the inverse susceptibility $\chi^{-1}(T)$ measured in different magnetic fields for the compound $La_{0.83}Sr_{0.17}Mn_{0.9}Fe_{0.05}Zn_{0.05}O_3$ is shown in the lower frame of Fig. 2. For H = 10 kOe at high T, $\chi^{-1}(T)$ varies linearly with T indicating a Curie–Weiss (CW) behavior. However, for the measurements done in lower dc fields (100 and 1000 Oe), $\chi^{-1}(T)$ shows a downward deviation from linearity below a temperature $T_G \sim 364$ K, significantly above T_C, which turns out to be the stronger the smaller the external field and is a typical signature of a Griffiths phase [22,25–31], where FM clusters coexist in the PM matrix. As the applied external magnetic field increases, the extent of deviation in magnetic susceptibility systematically diminishes until a pure CW behavior is observed. This is related to the fact that the magnetization of the PM matrix increases linearly with increasing H [22,25,30], while the contribution of the FM clusters is saturated already in small fields and, hence, for a sufficiently high field the PM susceptibility dominates over the weakly correlated FM clusters. The effective moment determined from the CW law as $\mu_{eff} = 5.29\ \mu_B$ is strongly enhanced compared to the theoretical value of $4.62\ \mu_B$ calculated from the square root of the sum of squared ionic moments of Mn^{3+} ($S = 2$), Mn^{4+} ($S = 3/2$), and Fe^{3+} ($S = 5/2$) weighted by the corresponding stoichiometric factors and using the spin-only g-value $g = 2$ [31]. This observation corroborates the general tendency for FM cluster formation in the PM phase in this compound.

Compared to $x = 0.05$, the $\chi^{-1}(T)$ curve of the Zn-free compound $x = 0$ (Fig. 3) does not exhibit any obvious downturn deviation from the CW law which could be a signature of a Griffiths phase. Note that the deviation to higher values from linearity below a certain temperature above T_C is due to fluctuations characteristic of usual ferromagnets. The

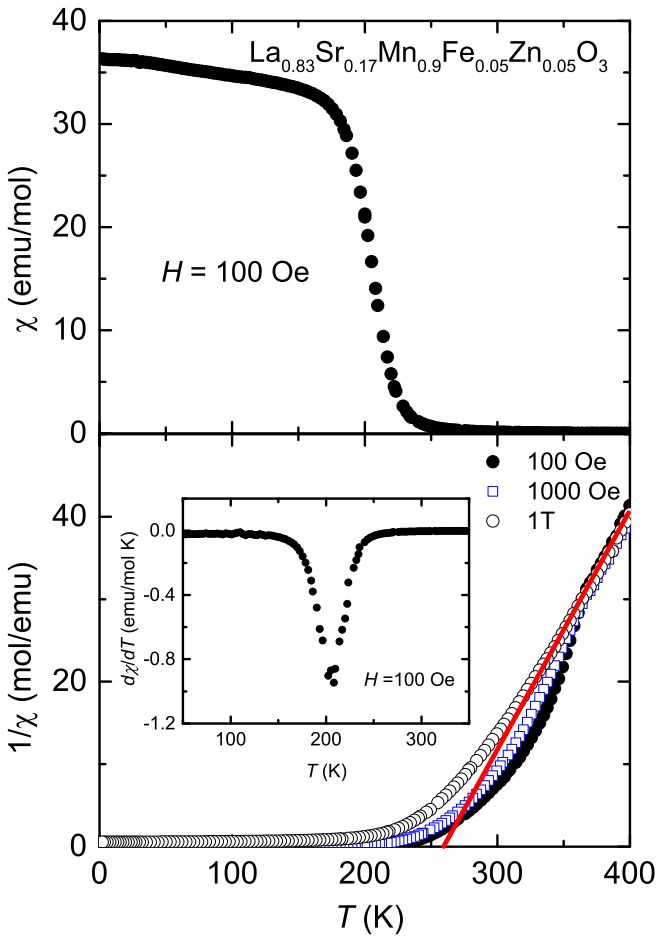

Fig. 2. Temperature dependence of dc magnetic susceptibility (upper frame) at H = 100 Oe and its inverse (lower frame) in $La_{0.83}Sr_{0.17}Mn_{0.9}Fe_{0.05}Zn_{0.05}O_3$ at 100 Oe, 1000 Oe, and 10 kOe. The solid line indicates a fit by a Curie–Weiss law. Inset (lower frame): The derivative of magnetic susceptibility $d\chi(T)/dT$ as a function of temperature.

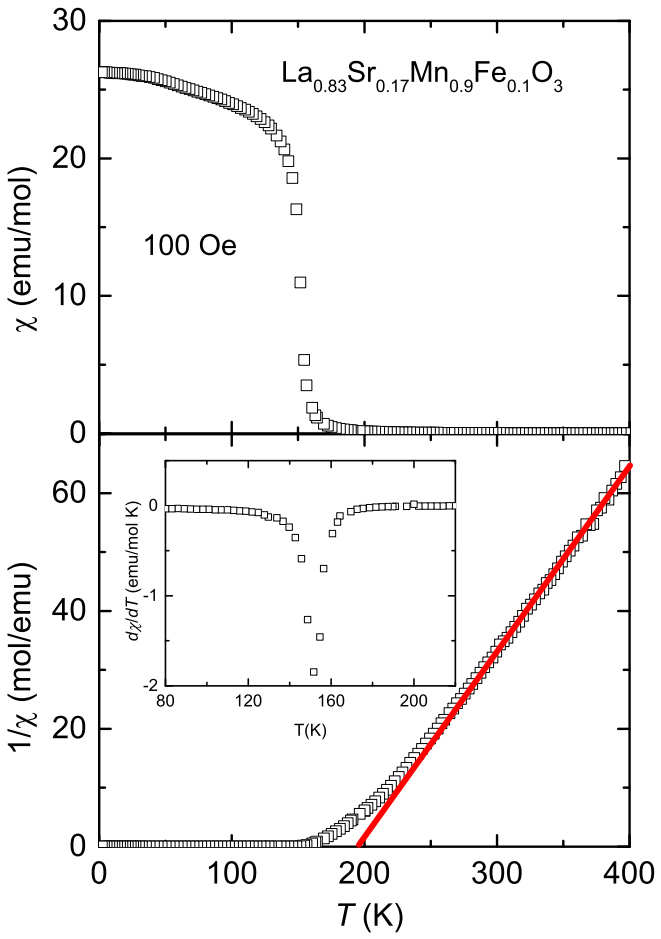

Fig. 3. Temperature dependence of dc magnetic susceptibility (upper frame) and its inverse (lower frame) in $La_{0.83}Sr_{0.17}Mn_{0.9}Fe_{0.1}O_3$ at H = 100 Oe. The solid line indicates a fit by a Curie–Weiss law. Inset (lower frame): The derivative of magnetic susceptibility $d\chi(T)/dT$ as a function of temperature.

Table 2
Saturation magnetization M_S at 2 K (in μ_B per formula unit), paramagnetic Curie-Weiss temperature Θ_{CW}(K), Curie temperature T_C of magnetic ordering and effective paramagnetic moment μ_{eff}(μ_B/f.u.) in $La_{0.83}Sr_{0.17}Mn_{0.9}Fe_{0.1-x}Zn_xO_3$ (x=0, x=0.05).

Compound	M_S (μ_B/f.u.) at 2 K	Θ_{CW} (K)	T_C (K)	μ_{eff} (μ_B/f.u.)
$x = 0.05$	3.30	259	208	5.29
$x = 0$	2.72	195	151	5.01

effective moment determined from the CW law as $\mu_{eff} = 5.01\ \mu_B$ is only slightly enhanced compared to the theoretical value of 4.86 μ_B. Thus, in the PM phase the tendency for FM cluster formation is significantly weaker for $x = 0$ than for $x = 0.05$.

Note that for a correct evaluation of the susceptibility it is necessary to estimate diamagnetic and van Vleck contributions and to check, if they have strong influence on the derived Curie–Weiss temperature and effective magnetic moment. Using the table given by [39] the diamagnetic susceptibility is calculated as $-65.49 \cdot 10^{-6}$ emu/mol for $x = 0$ and $-65.64 \cdot 10^{-6}$ emu/mol for $x = 0.05$. Comparable diamagnetic susceptibilities as well as the van Vleck susceptibilities were calculated by J. A. Souza et al. for related manganites [40]. As evident from that publication, the contributions of van Vleck and diamagnetic susceptibilities are opposite in sign and practically compensate each other resulting in a net contribution of about -10^{-5} emu/mol. This is three orders of magnitude smaller than the smallest experimental susceptibility value measured at 400 K and hence has no significant influence on the effective magnetic moment determined from the slope of the inverse susceptibility.

Fig. 4 shows the magnetization of both compounds under consideration as a function of magnetic field at 2 K. The magnetization for $x = 0.05$ reveals practically no hysteresis and immediately reaches the full saturation value at weak external fields. For $x = 0$ one observes a weak hysteresis and, above 10 kOe, the magnetization still slightly increases on increasing magnetic field. The saturation magnetization (M_S) in both compounds $La_{0.83}Sr_{0.17}Mn_{0.9}Fe_{0.05}Zn_{0.05}O_3$ and $La_{0.83}Sr_{0.17}Mn_{0.9}Fe_{0.1}O_3$ was obtained from a linear extrapolation of the high-field data [41] down to $1/H = 0$ as illustrated in the left inset of Fig. 4 and the values of $M_S(T = 2\,K)$ are deduced to be 3.30 μ_B and 2.72 μ_B, respectively. The latter value is in reasonable agreement with the corresponding theoretical magnetization of 2.93 μ_B, assuming ferromagnetically aligned Mn^{3+} and Mn^{4+} spins with the Fe^{3+} spins oriented antiparallel to the Mn spins and a g value close to $g = 2$. However, in the first case it is approximately at the average of parallel (3.63 μ_B) and antiparallel (3.13 μ_B) alignment. This indicates that disorder due to Zn doping induces parallel alignment of a part of the Fe spins.

3.2. Electron spin resonance

To further identify the presence of the Griffiths phase, we performed electron spin resonance (ESR) measurements on the $La_{0.83}Sr_{0.17}Mn_{0.9}Fe_{0.05}Zn_{0.05}O_3$ and $La_{0.83}Sr_{0.17}Mn_{0.9}Fe_{0.1}O_3$ samples. ESR is known

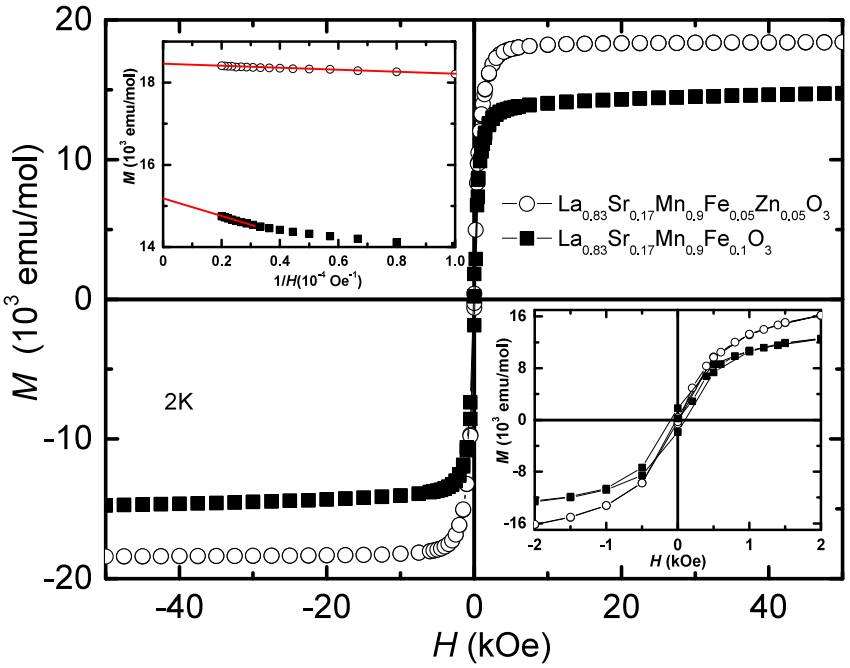

Fig. 4. Magnetization as a function of external field in $La_{0.83}Sr_{0.17}Mn_{0.9}Fe_{0.05}Zn_{0.05}O_3$ and $La_{0.83}Sr_{0.17}Mn_{0.9}Fe_{0.1}O_3$ at 2 K. Right inset: magnification at low fields. Left inset: magnetization as function of inverse field to determine the saturation magnetization.

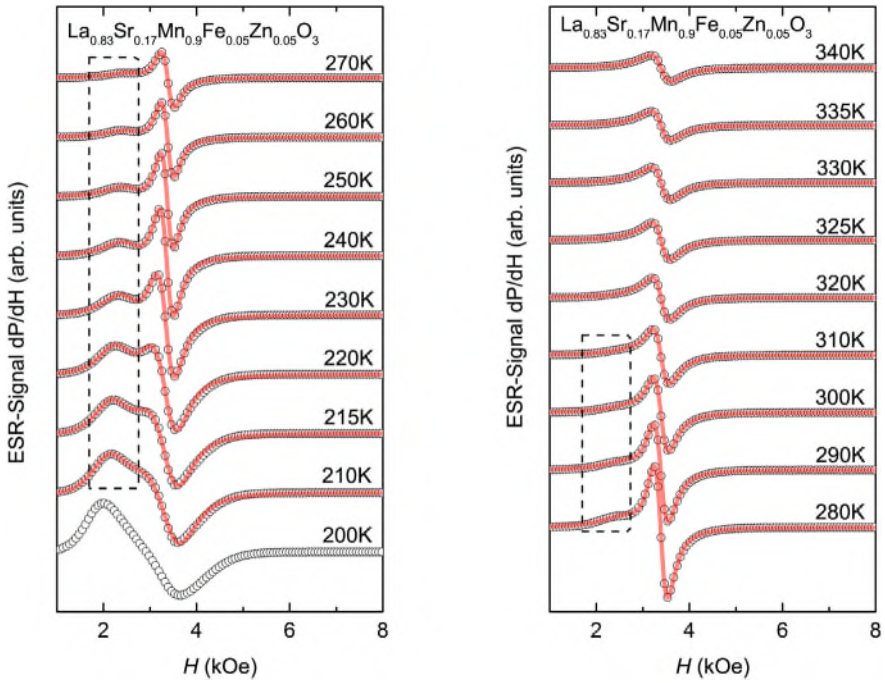

Fig. 5. ESR spectra of $La_{0.83}Sr_{0.17}Mn_{0.9}Fe_{0.05}Zn_{0.05}O_3$ at temperatures $200 \leq T \leq 340$ K.

as a powerful probe of spin dynamics and magnetic correlation in magnetic materials on a microscopic level. The signal of ESR is sensitive to the variation of localized environment of magnetic ions. Due to this feature, ESR has been also applied to identify the existence of Griffiths phases in some manganites, previously [20–25].

The ESR measurements have been performed using a BRUKER EMX-plus spectrometer working at X-band frequency (9.4 GHz) and equipped with a nitrogen gas-flow cryostat. Due to the lock-in technique with field modulation, the field derivative of the absorbed microwave power (dP/dH) is recorded as a function of the externally applied field. The observed ESR spectra of $La_{0.83}Sr_{0.17}Mn_{0.9}Fe_{0.1-x}Zn_xO_3$ are shown in Figs. 5 and 6 for $x = 0.05$ and $x = 0$, respectively.

Fig. 5 depicts a series of ESR spectra in a temperature range from 200 to 340 K across the phase transition regime (near and above T_C) for $x = 0.05$. At $T \geq 320$ K only a single PM resonance line shows up corresponding to the paramagnetic state. The g value $g = 1.96(1)$ slightly below the spin-only value 2 is typical for manganites. But at lower temperatures, the spectra do not only consist of a PM signal due to the majority of Mn^{3+} and Mn^{4+} spins, but also exhibit an intriguing FMR signal at lower resonance fields. Compared to PM resonance lines, the extra peak shows a notable difference which is strongly dependent

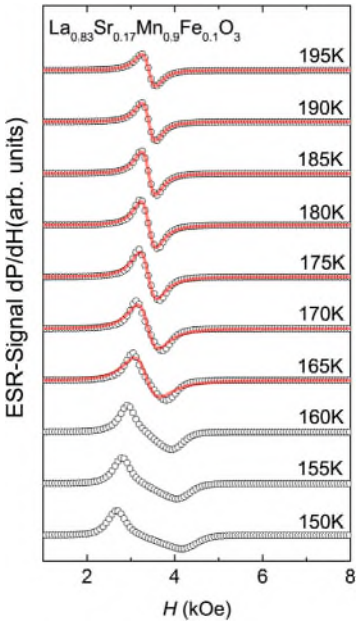

Fig. 6. ESR spectra of $La_{0.83}Sr_{0.17}Mn_{0.9}Fe_{0.1}O_3$ at temperatures $140 \le T \le 195$ K.

on temperature. As shown in the left and right part of Fig. 5, with the decrease of temperature, the intensity of this peak does not only increase but also the peak position gradually moves towards lower field regions. Therefore, from 320 K down to 210 K, two peaks coexist indicating that two different magnetic phases coexist in the system. At $T = 200$ K, both peaks finally merge into a single broad peak, which further shifts to lower field regions. In Fig. 2, at $T < 210$ K, one recognizes that the sample has undergone the PM–FM phase transition and all PM phase completely turns into the FM phase. Consequently, at $T < 210$ K, there remains only a single FMR peak to be detected. Thus, the temperature regime of coexisting ESR signals is in fair agreement with the GP regime derived from the susceptibility data.

For $La_{0.83}Sr_{0.17}Mn_{0.9}Fe_{0.1}O_3$ we observed a typical paramagnetic resonance line with a g-factor of $g = 1.96(1)$ in the temperature range $T > 165$ K, which is slightly higher than the onset temperature of the PM–FM transition in $\chi^{-1}(T)$ (Fig. 3). To lower temperature distortions of the resonance line show up on crossing T_C and the signal exhibits the characteristic shape of FMR in a polycrystal. The FMR shifts to lower field with decreasing temperature. Thus, the results of both $\chi^{-1}(T)$ and ESR show the normal PM–FM transition for $La_{0.83}Sr_{0.17}Mn_{0.9}Fe_{0.1}O_3$.

The full temperature dependences of the resonance fields H_{res} and linewidth data ΔH are summarized in Fig. 7. The splitting of the resonance fields in $La_{0.83}Sr_{0.17}Mn_{0.9}Fe_{0.05}Zn_{0.05}O_3$ is another key parameter for characterization of the coexistence of magnetic phases. The two curves in Fig. 7(a) depict the temperature dependence of the resonance fields for PM and FM peak, respectively. One can see that the position of the PM peak is almost constant at a magnetic field of $H = 3377$ Oe showing only a weak temperature dependence. The temperature dependence of the FMR field is well described by $H_{res} \propto (1 - T/T_G)^{1/2}$ with $T_G = 320$ K, which is somewhat lower than the value derived from the susceptibility data. This may be related to the fact that the precondition for the appearance of a well-defined FMR line is the formation of plate-like FM clusters, which is not necessarily fulfilled directly at the onset of the GP. Above the Curie temperature T_C, the linewidth ΔH of the PM line exhibits a minimum value of 233 Oe at a temperature of 255 K, diverges to lower temperature and increases approximately with linear slope (characteristic for relaxation via spin-phonon coupling [42]) to higher temperature, whereas ΔH of the FMR slightly increases with temperature and then decreases on approaching T_G. The temperature dependences of resonance field and linewidth of the PM peak of $La_{0.83}Sr_{0.17}Mn_{0.9}Fe_{0.1}O_3$ show a similar behavior above T_C as illustrated in Fig. 7(b).

Thus the ESR results support the findings of the magnetization measurements, i.e. for both compounds the typical behavior of the PM resonance on approaching a FM transition with resonance shift and line broadening due to enhanced internal demagnetization fields and critical fluctuations. For $x = 0.05$ the additional FMR line corroborates the coexistence of a FM phase in the PM regime. Zn^{2+} substitution enhances the number of Mn^{4+} spins and in turn FM Mn^{3+}-Mn^{4+} DE and at the same time increases disorder. Both effects favor the formation of a GP.

Table 3
Average hyperfine parameters of iron nuclei in $La_{0.83}Sr_{0.17}Mn_{0.9}Fe_{0.1-x}Zn_xO_3$ (x=0, x=0.05) samples at room temperature.

Compound	IS, mm/s	QS, mm/s
$x = 0.05$	0.35(4)	0.17(4)
$x = 0$	0.35(8)	0.15(2)

3.3. Mössbauer effect study

The Mössbauer measurements were carried out in a wide temperature range from room temperature to liquid nitrogen and liquid helium temperatures. The Mössbauer spectra of $La_{0.83}Sr_{0.17}Mn_{0.9}Fe_{0.1-x}Zn_xO_3$ at different temperatures are shown in Figs. 8 and 9 for $x = 0.05$ and $x = 0$, respectively. At room temperature, Mössbauer spectra of the samples under study consist of a slightly asymmetric doublet with a distribution of isomer (IS) and quadrupole shifts (ϵ). On the inset of Fig. 8 the distribution functions of the hyperfine parameters are given. They were restored by processing the experimental spectra with the SpectrRelax software [43]. The distribution function of Mössbauer parameters for the $La_{0.83}Sr_{0.17}Mn_{0.9}Fe_{0.05}Zn_{0.05}O_3$ sample shows the presence of two well-defined centers of iron ions with an area ratio close to 1:5 at room temperature.

Mathematical processing of the spectrum of the $La_{0.83}Sr_{0.17}Mn_{0.9}Fe_{0.1}O_3$ sample also reveals the presence of several centers of iron ions. Unfortunately, due to the low signal-to-noise ratio of the experimental spectra, the distribution functions of hyperfine parameters are determined with great uncertainty. This is especially noticeable for the spectra taken at low temperatures. Note that the lower signal-to-noise ratio results from the fact that the $x = 0$ sample was prepared with natural abundance of ^{57}Fe isotope, while for $x = 0.05$ we used ^{57}Fe enriched starting material. For this reason, we will not further consider the features of these distribution functions. We will focus on the temperature dependence of the average values of the hyperfine parameters. The values of isomer shift and quadrupole splitting (QS = 2ϵ) averaged over these centers are shown in Table 3.

As it is known, the isomer shift reflects the density of s-electrons in the iron nucleus, and it is sensitive to the oxidation state of iron and the coordination number. The average values of the isomer and quadrupole shift of Fe nuclei in the studied samples are 0.35 mm/s and 0.15–0.17 mm/s, respectively (Table 3). These values of the hyperfine parameters are typical for Fe^{3+} ions in the high-spin state, ($t_{2g}^3 e_g^2$) [44, 45]. The determined hyperfine parameters are in good agreement with the data reported in the literature for similar compounds [46,47]. The doping of La by a divalent cation, Sr, results partly in a change of the Mn valence from 3+ to 4+ [46], so that a part of Mn^{3+} is transformed into Mn^{4+}. In this case, it is reasonable to expect the manifestation of the presence of Fe^{4+} ions in the room-temperature Mössbauer spectra in the form of absorption features in the region of low and negative velocities. As can be seen from the distribution function for the isomer shift in Fig. 8, in this velocity region, the features due to Fe^{4+} ions are not observed. Probably, the preferable substitution of Fe^{3+} ions

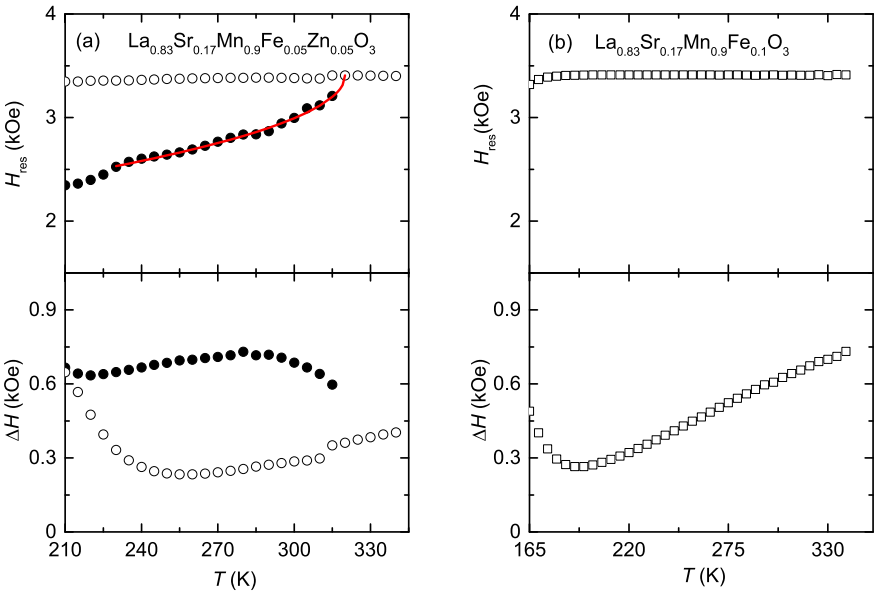

Fig. 7. (a) Temperature dependence of the resonance field H_{res} and linewidth ΔH in $La_{0.83}Sr_{0.17}Mn_{0.9}Fe_{0.05}Zn_{0.05}O_3$. The solid line describes the FMR shift (H_{res} = 3406 Oe - 1650 Oe$(1 - T/320\,K)^{1/2}$). (b) Temperature dependence of the resonance field H_{res} and linewidth ΔH in $La_{0.83}Sr_{0.17}Mn_{0.9}Fe_{0.1}O_3$.

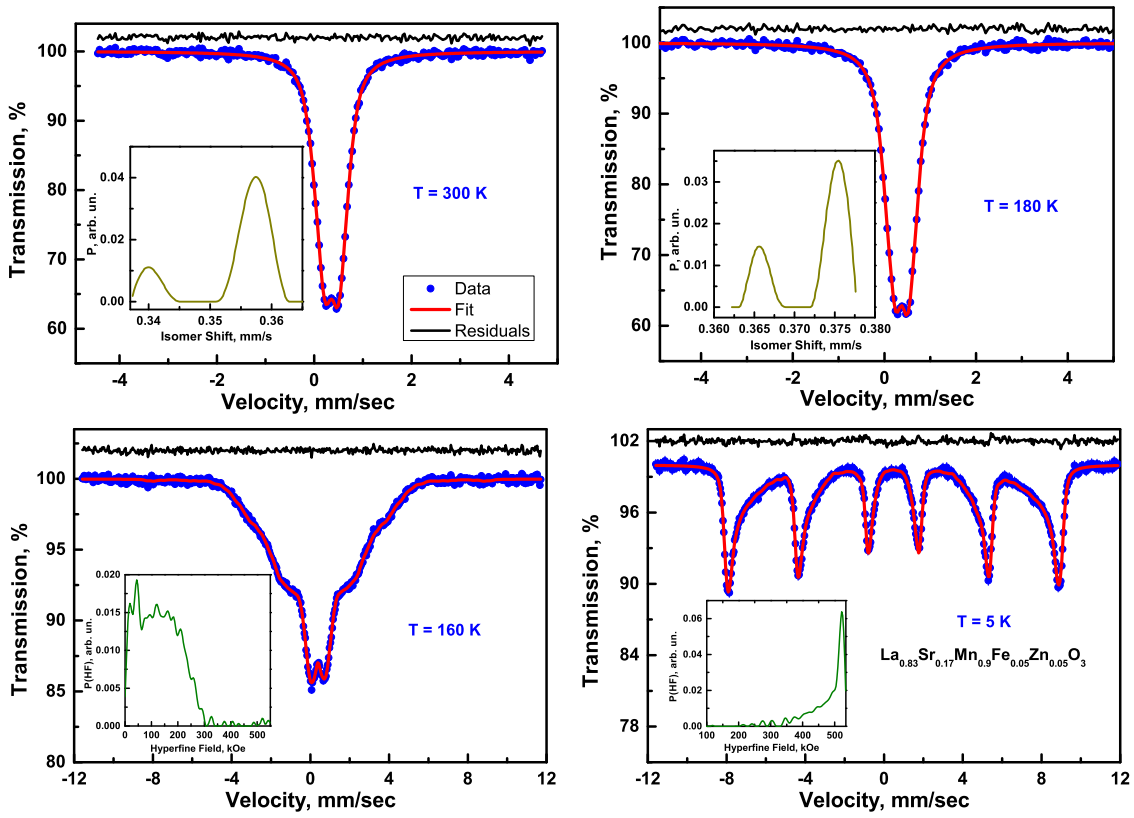

Fig. 8. Mössbauer spectra of the sample $La_{0.83}Sr_{0.17}Mn_{0.9}Fe_{0.05}Zn_{0.05}O_3$ at temperatures 300 K, 180 K, 160 K, and 5 K. Insets show the reconstructed distribution functions of hyperfine parameters, the difference between the experimental and approximating spectra in the range $\pm 3\sigma$ is shown above.

for Mn^{3+} ions is due to the identical ion size of these elements in the high-spin state.

When the temperature decreases, the Mössbauer spectra change dramatically, first acquiring the form of relaxation spectra with a wide distribution of hyperfine magnetic fields up to 300 kOe, and then, in the temperature range of liquid helium, the Mössbauer spectra are transformed into magnetic sextets (Fig. 8). At a temperature of 5 K, a noticeable peak is observed in the distribution of hyperfine fields at a value of 520 kOe and an extended tail towards low fields (insert in Fig. 8). The dependencies of the mean hyperfine magnetic field on the temperature for the studied samples are given in Fig. 10(a). According to Mössbauer measurements, magnetic ordering of the iron ions is achieved at a temperature of 180 K for $La_{0.83}Sr_{0.17}Mn_{0.9}Fe_{0.05}Zn_{0.05}O_3$ and at a temperature of 160 K for $La_{0.83}Sr_{0.17}Mn_{0.9}Fe_{0.1}O_3$.

The changes observed in the dependence of the mean quadrupole shift, ϵ, on temperature, also indicate the magnetic ordering of iron ions

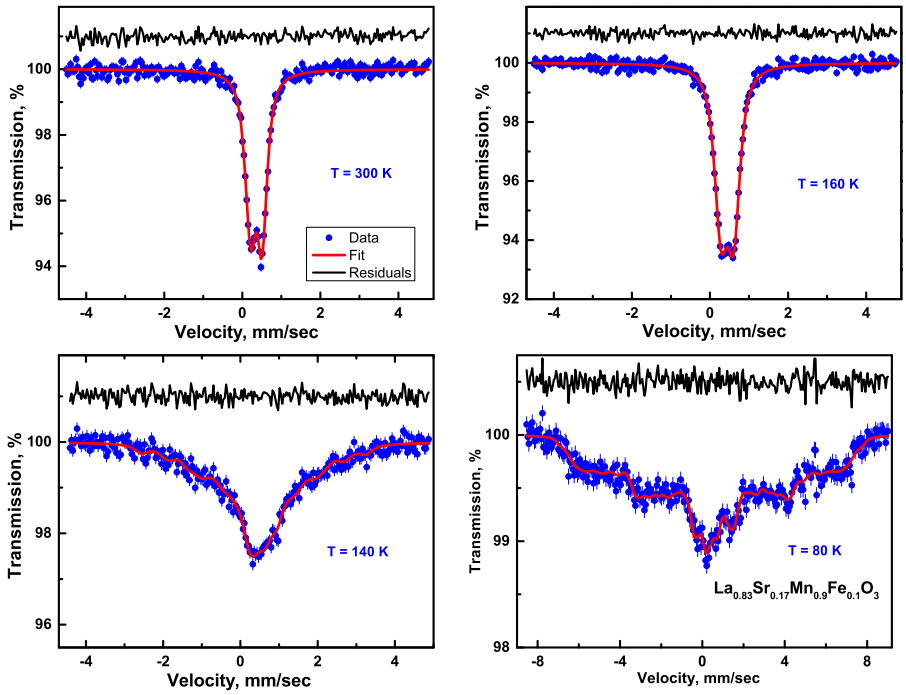

Fig. 9. Mössbauer spectra of the sample $La_{0.83}Sr_{0.17}Mn_{0.9}Fe_{0.1}O_3$ at temperatures 300 K, 160 K, 140 K, and 80 K. The difference between the experimental and approximating spectra in the range $\pm 3\sigma$ is shown above.

(Fig. 10(b)). When an ion is in a paramagnetic state, the splitting between the lines of the quadrupole doublet is determined by the product of the electric field gradient at the nucleus and the quadrupole moment of the nucleus, i.e $\Delta E_Q \approx 2\epsilon = e^2qQ/2$. In the case of magnetic ordering of resonant atoms and the appearance of a hyperfine magnetic field on the nucleus oriented with respect to the direction of the main axis of the quadrupole interaction tensor at some angle, the quadrupole shift is determined by the expression: $\epsilon = e^2qQ\cdot(3\cos^2\theta - 1)/8$, where q denotes the value of the electric field gradient (EFG), Q is the quadrupole moment of the nucleus, θ is the angle between the direction of the EFG and the hyperfine magnetic field. The sharp jump of the quadrupole shift observed in the region of the magnetic ordering temperature is probably due to the appearance of a hyperfine magnetic field on the nucleus at some angle to the direction of the EFG.

The temperature dependencies of the average isomer shift of iron ions of the studied samples are similar to each other and are mainly determined by the Doppler effect of the second order. Its value decreases monotonically with increasing temperature. The temperature dependencies of the average isomer shift of iron nuclei in $La_{0.83}Sr_{0.17}Mn_{0.9}Fe_{0.05}Zn_{0.05}O_3$ and $La_{0.83}Sr_{0.17}Mn_{0.9}Fe_{0.1}O_3$ are presented in Fig. 10(c). The solid line in Fig. 10(c) shows a curve that approximates, in the Debye approximation, the experimental values of the average isomer shift for the $La_{0.83}Sr_{0.17}Mn_{0.9}Fe_{0.05}Zn_{0.05}O_3$ sample. The best fit was achieved with a Debye temperature $\Theta_D = 342 \pm 38$ K.

It should be noted that the relaxation-like shape of the Mössbauer spectra and the specific temperature dependence of the average hyperfine field on the iron nuclei, which is unusual for conventional magnetically ordered materials, suggest that at low temperatures a complex magnetic correlation is formed in the samples under study.

4. Conclusions

In summary, we have investigated the magnetic behavior of polycrystalline samples of $La_{0.83}Sr_{0.17}Mn_{0.9}Fe_{0.1-x}Zn_xO_3$ ($x = 0$, $x = 0.05$). All samples show a clear FM–PM transition at T_C. The downward deviation of PM magnetization data from CW law together with the FMR line coexisting with the PM ESR signal suggests that the GP model is appropriate to describe the short-range ordered state for $x = 0.05$, while the upward deviation observed for $x = 0$ is caused by conventional fluctuations on approaching magnetic order. Mössbauer measurements show that in the studied perovskite-like manganites, doping with iron ions leads to the replacement of Mn^{3+} ions by Fe^{3+} ions in the high-spin state with the same ionic radius. Consequently, Fe ions occupy Mn sites without significant lattice distortions. However, this tendency can lead to phase separation and the formation of various magnetic clusters embedded in the paramagnetic matrix. The observed temperature dependence of the Mössbauer spectra of the compounds under study is typical of ferromagnetic clusters with a wide size distribution and magnetic correlation length. The temperature evolution of the spectra is probably determined by fluctuations of the iron magnetic moments due to the competition between the thermal energy and the energy of magnetic correlation.

Declaration of competing interest

The authors declare that they have no known competing financial interests or personal relationships that could have appeared to influence the work reported in this paper.

Acknowledgments

The authors thank Dana Vieweg for SQUID measurements. This work was partially supported by the Deutsche Forschungsgemeinschaft (DFG) within the Transregional Collaborative Research Center TRR 80 “From Electronic Correlations to Functionality”, project no. 107745057 (Augsburg, Munich, Stuttgart). Electron spin resonance measurements (I.V. Yatsyk, V.A. Shustov, R.M. Eremina) were performed with the financial support from the government assignment for FRC Kazan Scientific Center of RAS. The work of Z.Y. Seidov, M.J. Najafzade and I.N. Ibrahimov was supported by the Science Development Foundation under the President of the Republic Azerbaijan Grant EIF-BGM-4-RFTF-1/2017-21/03/1-M-03.

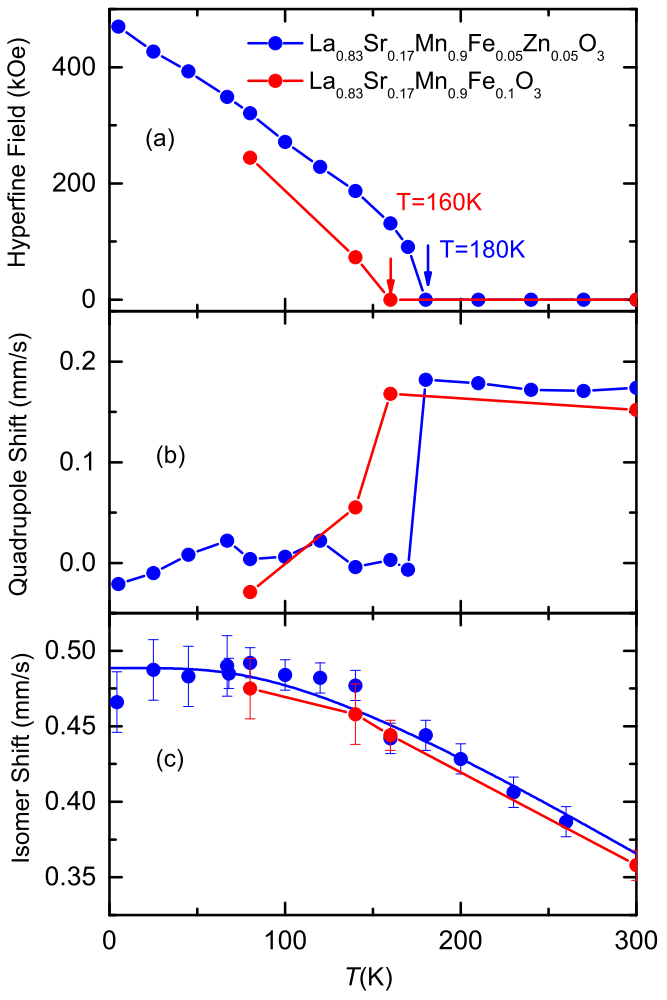

Fig. 10. Temperature dependence of Mössbauer parameters of ^{57}Fe in $La_{0.83}Sr_{0.17}Mn_{0.9}Fe_{0.05}Zn_{0.05}O_3$ and $La_{0.83}Sr_{0.17}Mn_{0.9}Fe_{0.1}O_3$: (a) the average hyperfine magnetic field on the iron nuclei. (b) the average quadrupole shift, ϵ, (c) the average isomer shift, δ, of the iron nuclei.

References

[1] P. Schiffer, A.P. Ramirez, W. Bao, S.W. Cheong, Low temperature magnetoresistance and the magnetic phase diagram of $La_{1-x}Ca_xMnO_3$, Phys. Rev. Lett. 75 (18) (1995) 3336, http://dx.doi.org/10.1103/PhysRevLett.75.3336.

[2] C.N.R. Rao, A. Arulraj, Giant magnetoresistance, charge-ordering and related aspects of manganase oxides, Curr. Opin. Solid State Mater. Sci. 3 (1) (1998) 23, http://dx.doi.org/10.1016/S1359-0286(98)80061-2.

[3] A. Moreo, S. Yunoki, E. Dagotto, Phase separation scenario for manganese oxides and related materials, Science 283 (1999) 2034, http://dx.doi.org/10.1126/science.283.5410.2034.

[4] N.G. Bebenin, R.I. Zainullina, V.V. Ustinov, Colossal magnetoresistance manganites, Phys.-Usp. 61 (8) (2018) 719, http://dx.doi.org/10.3367/UFNe.2017.07.038180.

[5] J. Hemberger, A. Krimmel, T. Kurz, H.-A. Krug von Nidda, V.Yu. Ivanov, A.A. Mukhin, A.M. Balbashov, A. Loidl, Structural, magnetic, and electrical properties of single-crystalline $La_{1-x}Sr_xMnO_3$ ($0.4 \le x \le 0.85$), Phys. Rev. B 66 (9) (2002) 094410, http://dx.doi.org/10.1103/PhysRevB.66.094410.

[6] J.-S. Zhou, J.B. Goodenough, Local structural distortions, orbital ordering, and ferromagnetism in underdoped $La_{1-x}Sr_xMnO_3$, Phys. Rev. B 91 (6) (2015) 064414, http://dx.doi.org/10.1103/PhysRevB.91.064414.

[7] E.L. Nagaev, Lanthanum manganites and other giant-magnetoresistance magnetic conductors, Phys.-Usp. 39 (8) (1996) 781, http://dx.doi.org/10.1070/PU1996v039n08ABEH000161.

[8] J.M.D. Coey, M. Viret, S. von Molnar, Mixed-valence manganites, Adv. Phys. 48 (2) (1999) 167, http://dx.doi.org/10.1080/000187399243455.

[9] E. Dagotto, T. Hotta, A. Moreo, Colossal magnetoresistant materials: the key role of phase separation, Phys. Rep. 344 (1–3) (2001) 1–153, http://dx.doi.org/10.1016/S0370-1573(00)00121-6.

[10] M.-H. Phan, S.-C. Yu, Review of the magnetocaloric effect in manganite materials, J. Magn. Magn. Mater. 308 (2) (2007) 325, http://dx.doi.org/10.1016/j.jmmm.2006.07.025.

[11] C. Zener, Interaction between the *d*-shells in the transition metals. II. ferromagnetic compounds of manganese with perovskite structure, Phys. Rev. 82 (3) (1951) 403, http://dx.doi.org/10.1103/PhysRev.82.403.

[12] E.O. Wollan, W.C. Koehler, Neutron diffraction study of the magnetic properties of the series of perovskite-type compounds $La_{1-x}Ca_xMnO_3$, Phys. Rev. 100 (2) (1955) 545, http://dx.doi.org/10.1103/PhysRev.100.545.

[13] R.B. Griffiths, Nonanalytic behavior above the critical point in a random Ising ferromagnet, Phys. Rev. Lett. 23 (1) (1969) 17–19, http://dx.doi.org/10.1103/PhysRevLett.23.17.

[14] V.M. Galitski, A. Kaminski, S. Das Sarma, Griffiths phase in diluted magnetic semiconductors, Phys. Rev. Lett. 92 (17) (2004) 177203, http://dx.doi.org/10.1103/PhysRevLett.92.177203.

[15] W. Jiang, X. Zhou, G. Williams, Y. Mukovskii, K. Glazyrin, Griffiths phase and critical behavior in single-crystal $La_{0.7}Ba_{0.3}MnO_3$: Phase diagram for $La_{1-x}Ba_xMnO_3$ ($x \le 0.33$), Phys. Rev. B 77 (6) (2008) 064424, http://dx.doi.org/10.1103/PhysRevB.77.064424.

[16] Z.W. Ouyang, V.K. Pecharsky, K.A. Gschneidner Jr., D.L. Schlagel, T.A. Lograsso, Short-range anisotropic ferromagnetic correlations in the paramagnetic and antiferromagnetic phases of Gd_5Ge_4, Phys. Rev. B 74 (9) (2006) 094404, http://dx.doi.org/10.1103/PhysRevB.74.094404.

[17] C. Magen, P.A. Algarabel, L. Morellon, J.P. Araújo, C. Ritter, M.R. Ibarra, A.M. Pereira, J.B. Sousa, Observation of a Griffiths-like phase in the magnetocaloric compound $Tb_5Si_2Ge_2$, Phys. Rev. Lett. 96 (16) (2006) 167201, http://dx.doi.org/10.1103/PhysRevLett.96.167201.

[18] N. Marcano, P.A. Algarabel, L. Fernández Barquín, J.P. Araujo, A.M. Pereira, J.H. Belo, C. Magen, L. Morellón, M.R. Ibarra, Cluster-glass dynamics of the Griffiths phase in $Tb_{5x}La_xSi_2Ge_2$, Phys. Rev. B 99 (2019) 055419, http://dx.doi.org/10.1103/PhysRevB.99.054419.

[19] S. Zhou, Y. Guo, J. Zhao, L. He, L. Shi, Size-induced Griffiths phase and second-order ferromagnetic transition in $Sm_{0.5}Sr_{0.5}MnO_3$ nanoparticles, J. Phys. Chem. C 115 (2011) 1535, http://dx.doi.org/10.1021/jp108553r.

[20] S.I. Andronenko, A.A. Rodionov, A.V. Fedorova, S.K. Misra, Electron paramagnetic resonance study of $(La_{0.33}Sm_{0.67})_{0.67}Sr_{0.33-x}Ba_xMnO_3$ ($x < 0.1$): Griffiths phase, J. Magn. Magn. Mater. 326 (2013) 151–156, http://dx.doi.org/10.1016/j.jmmm.2012.08.017.

[21] A.S. Kumar, R. Reddy K, A.K. Bhatnagar, Magnetization and ESR studies of $La_{0.67}(Ca_{1-x}Mg_x)_{0.33}MnO_3$ systems, J. Alloys Compd. 639 (2015) 139–144, http://dx.doi.org/10.1016/j.jallcom.2015.03.028.

[22] J. Deisenhofer, D. Braak, H.-A. Krug von Nidda, J. Hemberger, R.M. Eremina, V.A. Ivanshin, A.M. Balbashov, G. Jug, A. Loidl, T. Kimura, Y. Tokura, Observation of a Griffiths phase in paramagnetic $La_{1-x}Sr_xMnO_3$, Phys. Rev. Lett. 95 (12) (2005) 257202, http://dx.doi.org/10.1103/PhysRevLett.95.257202.

[23] R.M. Eremina, I.V. Yatsyk, Ya.M. Mukovskii, H.-A. Krug von Nidda, A. Loidl, Determination of the region of existence of ferromagnetic nanostructures in the paraphase of $La_{1-x}Ba_xMnO_3$ by the EPR method, JETP Lett. 85 (1) (2007) 51, http://dx.doi.org/10.1134/S0021364007010109.

[24] S.K. Misra, S.I. Andronenko, S. Asthana, D. Bahadur, A variable temperature EPR study of the manganites$(La_{1/3}Sm_{2/3})_{2/3}Sr_xBa_{0.33-x}MnO_3$ (x=0.0, 0.1, 0.2, 0.33): Small polaron hopping conductivity and Griffiths phase, J. Magn. Magn. Mater. 322 (19) (2010) 2902, http://dx.doi.org/10.1016/j.jmmm.2010.05.003.

[25] R.M. Eremina, I.I. Fazlizhanov, I.V. Yatsyk, K.R. Sharipov, A.V. Pyataev, H.-A. Krug von Nidda, N. Pascher, A. Loidl, K.V. Glazyrin, Ya.M. Mukovskii, Phase separation in paramagnetic $Eu_{0.6}La_{0.4-x}Sr_xMnO_3$, Phys. Rev. B 84 (6) (2011) 064410, http://dx.doi.org/10.1103/PhysRevB.84.064410.

[26] N. Rama, M.S. Ramachandra Rao, V. Sankaranarayanan, P. Majewski, S. Gepraegs, M. Opel, R. Gross, A-site-disorder-dependent percolative transport and griffiths phase in doped manganites, Phys. Rev. B 70 (22) (2004) 224424, http://dx.doi.org/10.1103/PhysRevB.70.224424.

[27] X. Zheng, T. Gao, W. Jing, X. Wang, Y. Liua, B. Chen, H. Dong, Z. Chen, S. Cao, C. Cai, V.V. Marchenkov, Evolution of Griffiths phase and spin reorientation in perovskite manganites, J. Magn. Magn. Mater. 491 (1) (2019) 165611, http://dx.doi.org/10.1016/j.jmmm.2019.165611.

[28] M.B. Salamon, P. Lin, S.H. Chun, Colossal magnetoresistance is a Griffiths singularity, Phys. Rev. Lett. 88 (19) (2002) 197203, http://dx.doi.org/10.1103/PhysRevLett.88.197203.

[29] M.B. Salamon, S.H. Chun, Griffiths singularities and magnetoresistive manganites, Phys. Rev. B 68 (1) (2003) 014411, http://dx.doi.org/10.1103/PhysRevB.68.014411.

[30] A.K. Pramanik, A. Banerjee, Griffiths phase and its evolution with Mn-site disorder in the half-doped manganite $Pr_{0.5}Sr_{0.5}Mn_{1-y}Ga_yO_3$ (y=0.0, 0.025, and 0.05), Phys. Rev. B 81 (2) (2010) 024431, http://dx.doi.org/10.1103/PhysRevB.81.024431.

[31] A.G. Silva, K.L. Salcedo Rodriguez, C.P. Contreras Medrano, G.S.G. Lourenco, M. Boldrin, E. Baggio-Saitovitch, L. Bufaical, Griffiths phase and spontaneous exchange bias in $La_{1.5}Sr_{0.5}CoMn_{0.5}Fe_{0.5}O_6$, J. Phys.: Condens. Matter 33 (6) (2020) 065804, http://dx.doi.org/10.1088/1361-648X/abc595.

[32] Y. Tokura, Y. Tomioka, Colossal magnetoresistive manganites, J. Magn. Magn. Mater. 200 (1) (1999) 1–23, http://dx.doi.org/10.1016/S0304-8853(99)00352-2.
[33] K.H. Ahn, X.W. Wu, K. Liu, C.L. Chien, Magnetic properties and colossal magnetoresistance of La(Ca)MnO_3 materials doped with Fe, Phys. Rev. B 54 (21) (1996) 15299, http://dx.doi.org/10.1103/physrevb.54.15299.
[34] G.F. Wang, Z.R. Zhao, H.L. Li, X.F. Zhang, Magnetocaloric effect and critical behavior in Fe-doped $La_{0.67}Sr_{0.33}Mn_{1-x}Fe_xO_3$ manganites, Ceram. Int. 42 (16) (2016) 18196–18203, http://dx.doi.org/10.1016/j.ceramint.2016.08.138.
[35] V.S. Zakhvalinskii, R. Laiho, A.V. Lashkul, K.G. Lisunov, E. Lähderanta, Yu S. Nekrasova, P.A. Petrenko, Phase separation, ferromagnetism and magnetic irreversibility in $La_{1-x}Sr_xMn_{1-y}Fe_yO_3$, J. Magn. Magn. Mater. 323 (16) (2011) 2186–2191, http://dx.doi.org/10.1016/j.jmmm.2011.03.028.
[36] J. Mizusaki, N. Mori, H. Takai, Y. Yonemura, H. Minamiue, H. Tagawa, M. Dokiya, H. Inaba, K. Naraya, T. Sasamoto, T. Hashimoto, Oxygen nonstoichiometry and defect equilibrium in the perovskite-type oxides $La_{1-x}Sr_xMnO_{3+d}$, Solid State Ion. 129 (1–4) (2000) 163–177, http://dx.doi.org/10.1016/S0167-2738(99)00323-9.
[37] Maud, Materials Analysis Using Diffraction, http://maud.radiographema.eu.
[38] D.V. Popov, T.P. Gavrilova, I.F. Gilmutdinov, M.A. Cherosov, V.A. Shustov, E.M. Moshkina, L.N. Bezmaternykh, R.M. Eremina, Magnetic properties of ludwigite $Mn_{2.25}Co_{0.75}BO_5$, J. Phys. Chem. Solids 148 (2021) 109695, http://dx.doi.org/10.1016/j.jpcs.2020.109695.
[39] G.A. Bain, J.F. Berry, Diamagnetic corrections and pascal's constants, J. Chem. Educ. 85 (4) (2008) 532–536, http://dx.doi.org/10.1021/ed085p532.
[40] J.A. Souza, J.J. Neumeier, R.K. Bollinger, B. McGuire, C.A.M. dos Santos, H. Terashita, Magnetic susceptibility and electrical resistivity of $LaMnO_3$, $CaMnO_3$, and $La_{1-x}Sr_xMnO_3$ ($0.13 \leq x \leq 0.45$) in the temperature range 300–900 K, Phys. Rev. B 76 (2) (2007) 024407, http://dx.doi.org/10.1103/PhysRevB.76.024407.
[41] S. Thota, S. Ghosh, Maruthi R, D.C. Joshi, R. Medwal, R.S. Rawat, M.S. Seehra, Magnetic ground state and exchange interactions in the Ising chain ferromagnet $CoNb_2O_6$, Phys. Rev. B 103 (6) (2021) 064415, http://dx.doi.org/10.1103/PhysRevB.103.064415.
[42] D.L. Huber, M.S. Seehra, Contribution of the spin-phonon interaction to the paramagnetic resonance linewidth of $CrBr_3$, J. Phys. Chem. Solids 36 (7–8) (1975) 723–725, http://dx.doi.org/10.1016/0022-3697(75)90094-3.
[43] M.E. Matsnev, V.S. Rusakov, SpectrRelax: an application for Mössbauer spectra modeling and fitting, AIP Conf. Proc. 1489 (2012) 178–185, http://dx.doi.org/10.1063/1.4759488.
[44] F. Menil, Systematic trends of the ^{57}Fe Mössbauer isomer shifts in (FeO_n) and (FeF_n) polyhedral. Evidence of a new correlation between the isomer shift and the inductive effect of the competing bond T-X (-Fe) (where X is O or F and T any element with a formal positive charge), J. Phys. Chem. Solids 46 (7) (1985) 763–789, http://dx.doi.org/10.1016/0022-3697(85)90001-0.
[45] E. Murad, J. Cashion, Mössbauer Spectroscopy of Environmental Materials and their Industrial Utilization, Springer Science+Business Media, New York, 2004, p. 418, http://dx.doi.org/10.1007/978-1-4419-9040-2.
[46] K. De, R. Ray, R.N. Panda, S. Giri, H. Nakamura, T. Kohara, The effect of Fe substitution on magnetic and transport properties of $LaMnO_3$, J. Magn. Magn. Mater. 288 (2005) 339–346, http://dx.doi.org/10.1016/j.jmmm.2004.09.118.
[47] M. Pissas, G. Kallias, E. Devlin, A. Simopoulos, D. Niarchos, Mössbauer study of $La_{0.75}Ca_{0.25}Mn_{0.98}Fe_{0.02}O_3$ compound, J. Appl. Phys. 81 (1997) 5770–5772, http://dx.doi.org/10.1063/1.364722.